Facile Preparation of Optically Transparent Film of Acetylated Cellulose Nanofiber-Reinforced Poly(Methyl Methacrylate) Utilizing Cosolvency in Aqueous Ethanol

Shogo Taira[a#], Ikuto Tanouchi[b], Shiori Suzuki[b,c]*, Tadahisa Iwata[c], and Yasumitsu Uraki[b]

[a] Research Institute for Chemical Process Technology, The National Institute of Advanced Industrial Science and Technology (AIST), Nigatake, 4-2-1, Miyagino-ku, Sendai 983-8551, Japan

[b] Research Faculty of Agriculture, Hokkaido University, Kita 9, Nishi 9, Kita-ku, Sapporo 060-8589, Japan.

[c] Department of Biomaterial Sciences, Graduate School of Agricultural and Life Sciences, The University of Tokyo, 1-1-1 Yayoi, Bunkyo-ku, Tokyo 113-8657, Japan

[#] Now at Forest Products Research Institute, Hokkaido Research Organization (HRO), 1-10, Nishikagura, Asahikawa 071-0198, Japan

* Correspondence; E-mail: suzuki-s@agr.hokudai.ac.jp, Tel: +81-11-706-2512

Abstract: Composite films of cellulose nanofibers (CNFs) and poly(methyl methacrylate) (PMMA) are fabricated typically by solution-casting using an organic solvent (e.g., chloroform) that can dissolve PMMA. However, the preparation of the casting dope using the previously reported method requires multistep procedures for the solvent exchange of the CNF suspension from water to the organic solvent. Here we developed a facile method utilizing the cosolvency of PMMA in aqueous ethanol (EtOH aq.) to fabricate an optically transparent CNF-reinforced PMMA film. In this study, an acetylated-CNF (Ac-CNF) was used as a hydrophobic filler for compatibility with a hydrophobic PMMA matrix. First, an appropriate amount of EtOH was added dropwise to Ac-CNF aq. suspension to adjust the EtOH concentration to 80 vol%. PMMA was then added to the solution and dissolved under heating above the upper critical solution temperature to yield a clear casting dope. The dope is cast at 65 ºC and then dried at 45 ºC for 24 h in a closed oven to obtain an Ac-CNF/PMMA composite film. The composite film with 1% Ac-CNFs exhibited high total-light transmittance (93%) and low haze (4.4%), while 1.3-times higher tensile strength and Young's modulus than the neat PMMA film, indicating the effective reinforcement of PMMA by the well-dispersed Ac-CNFs. Thus, this method enables the facile preparation of an Ac-CNF/PMMA composite film with excellent transparency and enhanced mechanical performance.

Keywords: hydrophobic cellulose nanofiber, acetylation, poly(methyl methacrylate), transparency, cosolvency

Introduction

Cellulose nanofibers (CNFs) have attracted much attention owing to their renewability and excellent properties, such as superior specific Young's modulus to steel and low coefficient of thermal expansion (Joshi et al. 2004; Abe et al. 2007; Isogai 2020). In general, the diameter of CNFs ranges between 3–20 nm, much smaller than the wavelengths of visible light (Moon et al. 2011; Daicho et al. 2018). Therefore, CNFs are suitable fillers for reinforcing optically functional materials such as epoxy and acrylic resins (Yano 2005). Poly(methyl methacrylate) (PMMA), also known as an acrylic glass, is essential industrial plastic owing to its excellent transparency, light weight, and shatter resistance (Ali et al. 2015; Hänig and Weller 2021). CNF-reinforcement of PMMA without impairing its transparency can afford the reduced thickness of PMMA-based window materials while meeting the required strength. This is advantageous in practical applications, such as transparent and pressure-resistant windows for aquarium and vehicles.

PMMA is typically molded via thermal melting at 170–260 ºC, depending on the product grade. Therefore, composite films with CNFs can be fabricated by melt-extrusion, followed by compression molding (Shih et al. 2018). However, such treatments at high temperatures often cause undesired aggregation and coloration (i.e., yellowing) of the CNFs (Taira et al. 2020; Niskanen et al. 2022), possibly reducing the transparency of the resulting films.

Solution casting is another molding method for PMMA using its good solvents, such as chloroform and *N*,*N*-dimethylformamide (DMF) (Patra et al. 2011). When blending PMMA and CNFs in a solution, the CNF suspension must be substituted from water with the organic solvent used for the PMMA dissolution, because CNFs are usually served in an aqueous medium. However, approximately more than 10 steps should be followed for the solvent exchange to avoid CNF aggregation. For instances, a casting dope containing 2,2,6,6-tetramethylpiperidine-1-oxyl (TEMPO)-oxidized CNFs (TOCN) and PMMA was prepared by stepwise solvent exchange of the TOCN suspension from water to DMF via acetone by repeated addition of each organic solvent, centrifugation, and homogenization, followed by mixing with the PMMA solution (Okita et al. 2011; Dong et al. 2015). Therefore, a facile method is required for blending aqueous CNF suspensions with PMMA.

To prepare a casting dope without tedious solvent exchange, a new solvent system should be developed in place of the methods using organic solvents mentioned above. PMMA is insoluble in water and alcohols but specifically dissolves in binary solutions exceeding the upper critical solution temperatures (UCSTs) (Cowie et al. 1987) owing to the cosolvency effect (Wolf and Molinari 1973; Cowie and McEwen 1974; McNaught et al. 1997). Based on this phenomenon, it is hypothesized that a CNF/PMMA dope can be prepared simply by adding ethanol (EtOH) to the CNF aqueous suspension and subsequent dissolving PMMA under heating above the UCST.

This study aims to develop a facile method for preparing an optically transparent film of CNF-reinforced PMMA. Herein, acetylated-CNFs (Ac-CNFs) with a degree of substitution (DS) of 2.24 (Taira et al. 2020) are used as hydrophobic fillers that should be compatible with a hydrophobic PMMA matrix. In this study, a new method based on the cosolvency of PMMA in aqueous EtOH (EtOH aq.) was used to

blend the as-prepared Ac-CNF aq. suspension and PMMA. For the prepared dope, appropriate conditions for casting and drying to fabricate the film were further investigated. The transparency and tensile properties of the resultant Ac-CNF/PMMA composite film were evaluated in comparisons with those of the neat PMMA film and other composite films containing commercially available CNFs. Specifically, TOCN and carboxymethylated CNFs (CM-CNFs) were used as the hydrophilic references. Each composite film was prepared similarly to that of Ac-CNFs.

Materials and methods

Materials

PMMA (product grade: MD, ACRYPET^{TM}) was purchased from Mitsubishi Chemical Co. A TOCN and CM-CNF aq. suspension with each 1 wt% consistency was kindly provided by Nippon Paper Industries Co. Ltd. An Ac-CNF aq. suspension was prepared as previously described (Taira et al. 2020). Briefly, 40 g of cellulose powder (KC flock W-50GK, Nippon Paper Industries Co. Ltd.; average particle size of 45 μm, 50–90 mesh, apparent density of 0.33 g cm^{-3} in the company catalog) was acetylated using 240 g of acetic anhydride and 6 g of sulfuric acid under a heterogeneous condition in 750 g of a binary solution (toluene: acetic acid = 9:1, w/w). The resulting cellulose acetate (CA) was then defibrillated and desulfated. The obtained CA aq. suspension was dialyzed in distilled water for 3 days, and the concentrated solution was used as an Ac-CNF aq. suspension with 0.69 wt% consistency. Other chemicals were obtained from commercial sources and used as received.

Preparation of neat PMMA film

PMMA (9 g) was dissolved in 150 mL of 80 vol% EtOH aq. at 65 ºC with stirring for 12 h. A total of 20 mL of the obtained clear solution was transferred into glass Petri dishes preheated at 65 ºC for 1 h. In precise, each 5 mL was poured into four dishes with an inner diameter of 48 mm, while each 10 mL was poured into two dishes with an inner diameter of 87 mm. The casting dope was subsequently dried at 45 ºC for 24 h in a completely closed square-type oven with inner dimensions of 30×30×30 cm (ADP300, Yamato Scientific Co. Ltd.). Thereby, two types of neat PMMA films with the different diameters (48 and 87 mm) and a constant thickness (c.a. 100 μm) were fabricated for optical measurements and tensile tests, respectively.

Preparation of Ac-CNF, TOCN, and CM-CNF/PMMA composite films

The preparation scheme of an Ac-CNF/PMMA composite film is shown in **Fig. 1**. Ac-CNF aq. suspension (0.69 wt%, 13 g) was transferred into a 200-mL round flask and diluted with Milli-Q water (17 g) under stirring for 30 min at room temperature (r.t., 25 ºC). EtOH (120 mL) was added dropwise to the Ac-CNF aq. suspension under stirring at r.t. while taking approximately 4 h. PMMA (9 g) was then added to the flask, to which a reflux condenser was attached. The PMMA was completely dissolved at 65 ºC under

stirring for 12 h to obtain a clear solution consisting of 6 w/v% of PMMA, 0.06 w/v% of Ac-CNFs, and 150 mL of 80 vol% EtOH aq. After heating at 70 ºC for 1 h, a total of 20 mL of the resultant solution was poured into the preheated four or two glass Petri dishes and then dried at 45 ºC for 24 h in a closed oven. The resulting film was peeled off from the dishes to yield a composite film with 1% Ac-CNFs based on the mass of PMMA.

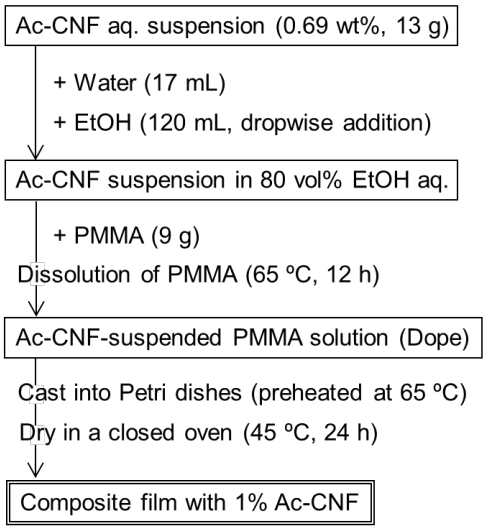

Fig. 1. Preparation scheme of a PMMA-based cast film containing with 1% Ac-CNFs.

Similarly, TOCN/PMMA and CM-CNF/PMMA composite films with the CNF loading of 1% for each were prepared. Each CNF aq. suspension (1 wt%, 9 g) was diluted with Milli-Q water (21 g), and EtOH (120 mL) was added dropwise. PMMA (9 g) was added to the resulting CNF suspension in 80 vol% EtOH aq. and dissolved at 65 ºC for 12 h under stirring. The CNF/PMMA dope was subsequently cast and dried in the similar manner to prepare the Ac-CNF/PMMA composite film, yielding TOCN/PMMA and CM-CNF/PMMA composite films.

Scanning electron microscopic observation.

After the film sample was coated with Pt for 120 s using an ion sputter (E-1030, Hitachi High-Tech Co. Ltd.), scanning electron microscopy (SEM) images of the film surface and cross-section were acquired with a field emission scanning electron microscope (JSM-6301F, JEOL) operating at an accelerating voltage of 5 kV.

UV and haze measurements

UV-vis transmittance of each film in the wavelength range from 200 to 800 nm was measured using a UV spectrophotometer (UV-1800, SHIMADZU Co. Ltd.). The haze of each film with a thickness of approximately 100 μm was determined using an HZ-V3 instrument (Suga Test Instruments Co. Ltd.), in which a D65 light source was applied. According to JIS K7136, an optic standard plate (No. 2011-042-1, Suga Test Instruments Co. Ltd.; haze = 1.24%, total transmittance = 90.90%) was used for the calibration

of the instrument. The total transmittance (T_T), consisting of the parallel transmittance and diffuse transmittance (T_D), and T_D were measured three points for each film and then averaged. The haze value (%) was calculated as follows:

$$\text{Haze } \% = (T_D / T_T) \times 100 \quad \cdots \quad \textbf{(Eq. 1)}$$

Tensile tests

Tensile tests were conducted at r.t. using a universal testing machine (SHIMADZU AGS-500D Autograph, Shimadzu Co. Ltd.). Strip-shaped specimens (50×10 mm) were prepared from each film using a hot cutter. The initial gauge length was 30 mm, and the crosshead speed was 1 mm min^{-1}. The tensile strength and Young's modulus were estimated from the obtained stress–strain (S–S) curves and averaged for three specimens.

Thermogravimetric analysis

Thermogravimetric analysis (TGA) was performed using a TG-DTA2000S apparatus (MAC Science Co. Ltd.) at a temperature range of 50–500 °C, employing a heating rate of 10 °C min^{-1} under a N_2 flow at 150 mL min^{-1}. Each film sample was vacuum dried at 50 ºC for 24 h to remove the moisture, and 10 mg of the dried sample was used for the measurements. The thermal decomposition temperature ($T_{d\text{-}5\%}$) was determined as the onset of significant (≥5%) weight loss.

Results and discussion

Dope Preparation using 80 vol% EtOH aq.

UCST of PMMA in EtOH aq. has been reported to depend on the EtOH concentration (McNaught et al. 1997; Cowie et al. 1987), and the lowest UCST (c.a. 40 ºC) was observed in the 80 vol%. In our preliminary experiments, 6 w/v% of PMMA pellets (**Fig. S1a**) were completely dissolved in the 80 vol% EtOH aq. at 65 ºC (**Fig. S1b**) that was applied at a sufficiently higher temperature than the reported UCST.

To prepare the Ac-CNF/PMMA casting dope, an Ac-CNF suspension in 80 vol% EtOH aq. was obtained by simply adding an appropriate amount of EtOH to the as-prepared Ac-CNF aq. suspension. In the first attempt, EtOH was added at once to the Ac-CNF aq. suspension; however, visible aggregates were formed in the resulting solution (**Fig. S2a**). Then, EtOH was added dropwise with stirring at r.t. Thereafter, the Ac-CNFs remained in good dispersion in the 80 vol% EtOH aq. (**Fig. S2b**), which was also confirmed by TEM (**Fig. S4**). PMMA (6 w/v%) was subsequently added to the prepared 0.06 w/v% Ac-CNF suspension in 80 vol% EtOH aq., and then dissolved at 65 ºC under stirring for 12 h. Finally, a clear casting dope containing 1% Ac-CNFs based on the mass of PMMA was obtained.

The TOCN and CM-CNF suspensions in the 80 vol% EtOH aq. were also prepared by dropwise addition of EtOH into the original aq. suspensions, because the addition of EtOH at once caused the

apparent aggregation of CNFs (**Fig. S3**) as well as Ac-CNFs. In the similar manner to the Ac-CNF dope, PMMA (6 w/v%) was then added to the suspension, yielding the clear casting dopes containing 1% of each CNF.

Casting the prepared dope above UCST

First, the prepared Ac-CNF/PMMA dope was cast onto a glass plate at r.t.; however, the clear solution quickly turned opaque, resulting in a white-turbid film after complete drying (**Fig. S5a**). This was due to the phase transition of PMMA, which was exposed onto the glass below UCST (**Fig. S1c**) (Nakata 1995; Yoneda et al. 2014). As a subsequent attempt, the dope was cast onto a glass plate under heating at 70 ºC. However, many bubbles were generated immediately and remained in the film (**Fig. S5b**), possibly due to the casting temperature being close to the boiling point (b.p.) of EtOH, which induces its rapid evaporation. Accordingly, the dope was poured into the glass Petri dishes preheated at 65 ºC. This temperature was above UCST and adequately lower than the b.p.; thus, the applied procedure successfully allowed the casting of the dope without turbidity or bubble generation.

Drying of the cast dope in a closed system for film fabrication

Herein, a PMMA dope in 80 vol% EtOH aq. was used to investigate the drying condition for film fabrication. As a first attempt, the PMMA dope, cast similarly as mentioned above, was subjected to vacuum drying at 65 ºC. However, a cloudy film was generated, possibly because the decrease in the EtOH concentration of the dope during vacuum drying increased the UCST of PMMA (Cowie et al. 1987), causing partial precipitation. In the second attempt, the cast dope was placed in a completely closed oven to prevent the release of EtOH vapor during drying. It was dried at 65 ºC for 12 h at ambient pressure to obtain a transparent film. However, wrinkles formed on the film surface (**Fig. S6**). In the third attempt, the cast dope was dried at 45 ºC for 24 h to slow solvent evaporation. Consequently, a neat PMMA film with a smooth surface was successfully fabricated (**Fig. 2a**).

The aforementioned drying condition was applied to the Ac-CNF/PMMA dope to fabricate the composite film. The resulting Ac-CNF/PMMA composite film (**Fig. 2b**) was uniform and transparent, comparable to the neat PMMA film (**Fig. 2a**). In contrast, when this drying condition was applied to dopes containing other CNFs (i.e., TOCN and CM-CNFs), the resultant composite films had relatively rough and wavy surfaces (**Fig. 2c,d**). SEM observations of the TOCN/PMMA and CM-CNF/PMMA composite films also revealed the surface roughness in the μm-order (**Fig. 3**). There are two possible reasons for this roughness: 1) microphase separation between the uniform phase of PMMA and the aggregate phase of PMMA around the hydrophilic CNFs, and 2) suppression of water evaporation during the drying process by hydrophilic CNFs in the dopes, resulting in the PMMA domains with different densities.

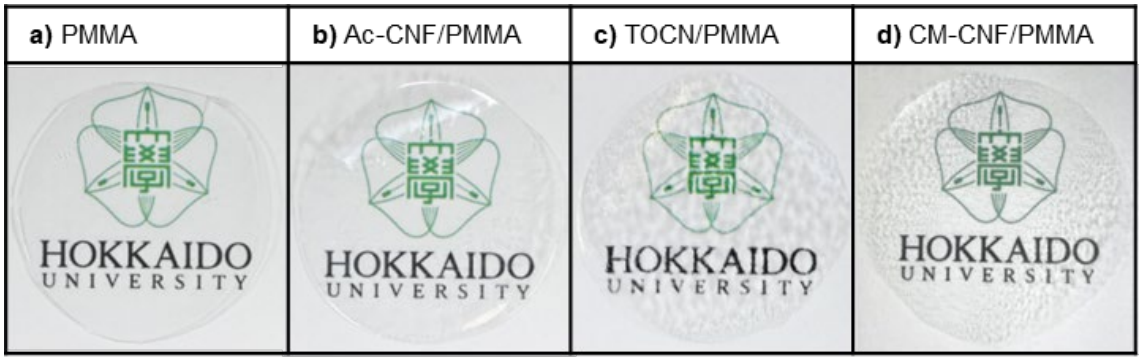

Fig. 2. a) Neat PMMA film and composite films with 1% of b) Ac-CNFs, c) TOCN, and d) CM-CNFs. All the films were prepared from each dope in 80 vol% EtOH aq., followed by casting at 65 °C and subsequent drying at 45 °C for 24 h in a closed oven.

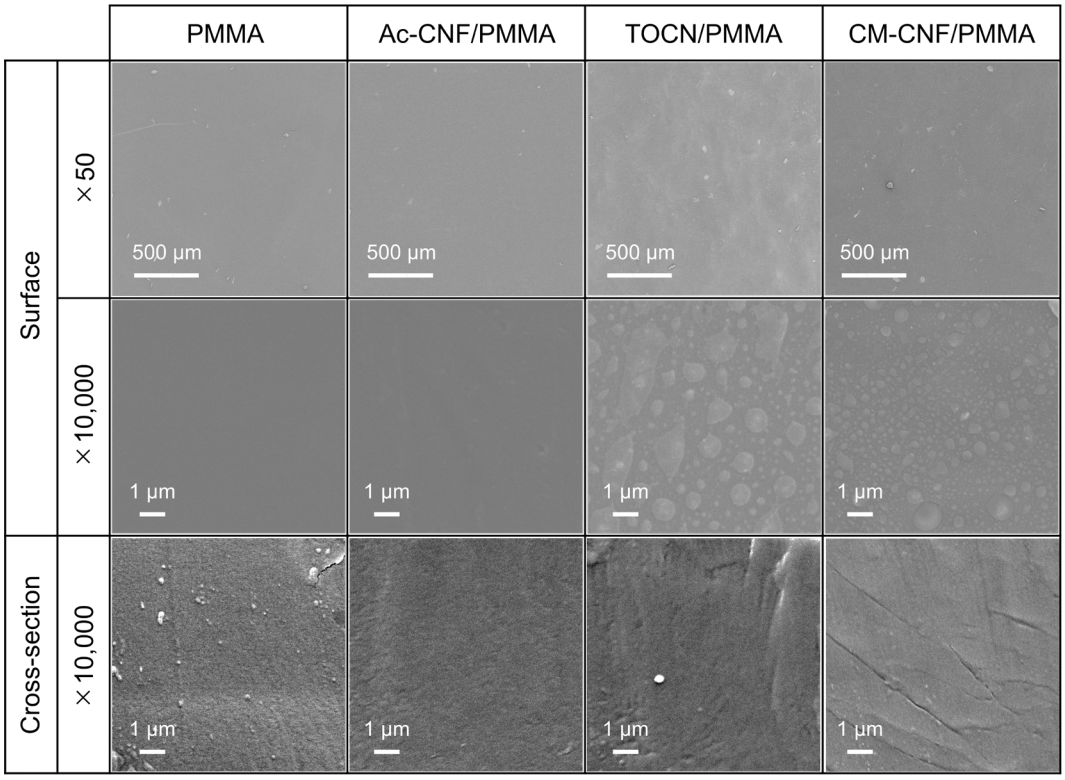

Fig. 3. SEM images of the surfaces and cross-sections of neat PMMA and composite films with 1% Ac-CNFs, TOCN, and CM-CNFs.

Transparency of CNF/PMMA composite films

To evaluate the transparency of the PMMA-based films, the UV-vis transmittance of each film was measured (**Fig. S7**). The magnified spectra in the visible light region are shown in **Fig. 4**. The neat PMMA film exhibited a consistently high transmittance of approximately 92%, consistent with previously reported films prepared by solution casting using organic solvents (Guo et al. 2011; Heiba et al. 2016). On the other

hand, the transmittance of the Ac-CNF/PMMA film increased from 87.1 to 90.8% as the wavelength increased, suggesting an acceptably high transparency. Although the CM-CNF/PMMA film exhibited a similar tendency, its maximum transmittance was 90.0% at 800 nm. In contrast, the TOCN/PMMA film showed the lowest transmittance among all the films, which might be due to light scattering of the TOCN aggregates in the film (Fukuzumi et al. 2008).

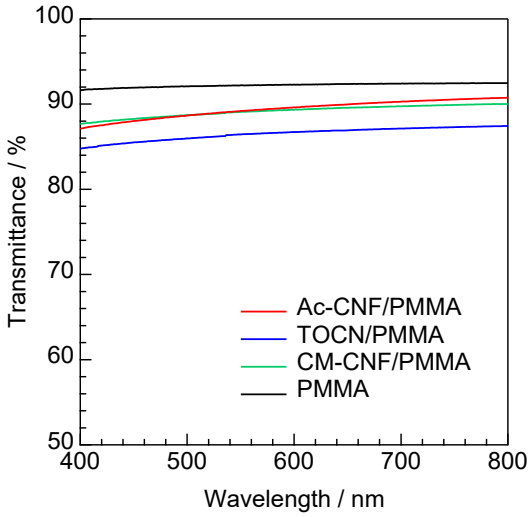

Fig. 4. Visible light transmittances of neat PMMA film and composite films with 1% Ac-CNFs, TOCN, and CM-CNFs.

The film transparency was further assessed based on the total transmittance (T_T) and haze of each film. As shown in **Table 1**, the Ac-CNF/PMMA film exhibited a high T_T and low haze, comparable to those of the neat PMMA film. Therefore, it can be considered that this composite film successfully retained the high transparency of PMMA. In contrast, the TOCN and CM-CNF/PMMA composite films showed lower T_T than the neat PMMA film, and their haze values were also much higher. The haze value of the CM-CNF/PMMA film was twice as high as that of the Ac-CNF/PMMA film, although the average thickness of the CM-CNF film was approximately 20 μm thinner (**Table 1**). Such high haze might be attributed to the similar reasons for the roughness of the film surface as mentioned above.

Table 1 Total light transmittance (T_T) and haze of neat PMMA film and composite films with 1% Ac-CNFs, TOCN, and CM-CNFs

Entry	Film thickness / μm	T_T / %	Haze / %
PMMA	111 ± 7	92 ± 0.1	1.8 ± 0.2
Ac-CNF/PMMA	117 ± 7	93 ± 0.0	4.4 ± 0.1
TOCN/PMMA	116 ± 7	88 ± 0.1	11.9 ± 0.5
CM-CNF/PMMA	93 ± 3	90 ± 0.1	8.7 ± 0.2

When compared with previous composite films, all the composite films prepared from the 80 vol% EtOH aq. dopes in this study show the comparable transmittance at the wavelength of 600 nm to those of the CNF/PMMA composite films prepared via conventional solvent exchange method (**Table 2**). Furthermore, the Ac-CNF/PMMA exhibited much higher transparency with haze of 4.4% (**Table 1**) than the surface-acetylated CNF/PMMA film with haze of 25.5% (Jamaluddin et al. 2021), even accounting that its film thickness (194 μm) was thicker than that of the Ac-CNF/PMMA (117 μm). The comparisons indicate that this film fabrication utilizing cosolvency in EtOH aq. is a facile method for the fabrication of CNF/PMMA composite films with high transparency.

Table 2 Comparison of transparency of CNF/PMMA composite films and reinforcing effects of 1% CNFs on the tensile strength of PMMA

CNF	Transmittance at 600 nm / %	Tensile strength / MPa		Increment [e] / times	Casting solvent	Reference
		neat PMMA	CNF/PMMA composite			
Ac-CNF [a]	90	34.5 ± 0.5	46.2 ± 1.4	1.34	80 vol% EtOH aq.	This study
TOCN	87		32.6 ± 0.4	0.94		
CM-CNF	89		39.8 ± 0.6	1.15		
TOCN	91 [f]	53.2 ± 5.6	45.9 ± 2.4	0.86	DMF	Dong et el. (2015)
TOCN	92	52.9 ± 2.0	58.1 ± 1.2	1.10	DMF	Fujisawa et al. (2018)
Ac-CNF [b]	74 (16 [g])	33.1 ± 0.5	40.0 ± 7.7	1.21	Chloroform	Jamaluddin et al. (2021)
Pr-CNF [c]	72 (17 [g])		41.2 ± 2.9	1.24		
MPTMS-CNF [d]	85	22.1 ± 0.6	19.8 ± 0.6	0.90	Chloroform	Kono et al. (2022)

[a] Ac-CNFs used in this study; DS = 2.24 according to our previous report (Taira et al. 2020). [b] Surface acetylated CNFs; DS = 0.88. [c] Surface propionylated CNFs; DS = 0.62. [d] 3-(Methacryloyloxy)propyltrimethoxysilylane (MPTMS)-modified bacterial CNF; DS = 0.60. [e] Increment (or decrement) is defined as the ratio of the tensile strength of each CNF/PMMA composite film to that of the neat PMMA film. [f] At the wavelength of 550 nm. [g] Reported haze values.

Reinforcing effects of CNFs on the mechanical and thermal properties of PMMA

The mechanical properties of the CNF/PMMA composite films were investigated by tensile testing in comparison with those of the neat PMMA film. A representative S–S curve for each film is shown in **Fig. 5a**, and the average values of the strain energy density at failure (i.e., toughness) and Young's modulus are summarized in **Fig. 5b**.

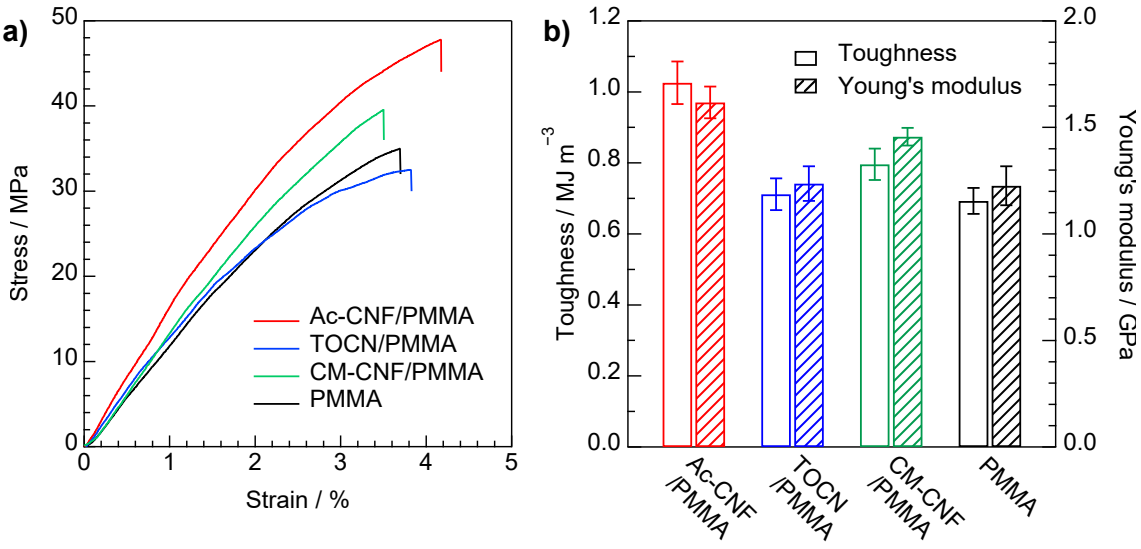

Fig. 5. (a) Representative S–S curves of neat PMMA film and composite films with 1% Ac-CNFs, TOCN, and CM-CNFs, obtained by tensile testing and (b) the averaged toughness and Young's modulus (n=3).

The glassy PMMA film showed a typical brittle fracture with an elongation at break of 3.6%, consistent with a previous report (Dong et al. 2015). Incorporation of only 1% of Ac-CNF increased the elongation at break to 4.1% (**Fig. 5a**). This result suggests good compatibility between the Ac-CNF and PMMA. Furthermore, the tensile strength and Young's modulus also increased 1.3 times those of the neat PMMA film. Thereby, the toughness (1.0 MJ m^{-3}) is 1.5 times greater than the neat PMMA film (0.7 MJ m^{-3}) (**Fig. 5b**). This effective reinforcement suggests that a good dispersion of Ac-CNFs in the PMMA matrix can suppress the deformation and breakage of the entire film. However, further increasing the Ac-CNF load to 5% resulted in a brittle behavior with a lower tensile strength than that of the neat PMMA film (**Fig. S8**). When loading 1% of Ac-CNFs, a uniform phase was formed in the composite film, enabling the effective transfer of strain energy from the matrix to the filler (Rusli et al. 2010; Wang et al. 2017). On the other hand, 5% loading would cause two domains of the aggregates of Ac-CNFs and PMMA matrix, resulting in the stress concentration at the interface (**Fig. S9**).

The S–S curve of the TOCN/PMMA composite film was similar to that of the neat PMMA film, but the tensile strength at break was reduced by ~6% (**Fig. 5a**). This result suggests that the stress concentration of the TOCN aggregates occurred in the composite film. In contrast, the tensile strength and Young's modulus of the CM-CNF/PMMA composite film were 1.2- and 1.1-fold higher than those of the neat

PMMA film, respectively, although the elongation at break slightly decreased. Consequently, the toughness (0.8 MJ m^{-3}) improved 1.1 times higher than the neat PMMA film (**Fig. 5b**), but the reinforcement effect of 1% CM-CNFs is inferior to that of the 1% Ac-CNFs.

Here, the reinforcement effects of CNFs in this study were compared with those in the previous reports (**Table 2**). In the solvent exchange method using DMF (Dong et al. 2015), when loading 1 wt% TOCN, the tensile strength of the composite film was reduced than that of the neat PMMA film, suggesting no reinforcement effect. However, at the 5 wt.% loading, the slight improvement (1.06 times) of the tensile strength was observed. On the other hand, Fujisawa and coworkers confirmed the reinforcement effect (1.10 times) of TOCN with 1 vol% loading (Fujisawa et al. 2018). Jamaluddin et al. reported that surface-acetylated (DS = 0.88) and propionylated (DS = 0.62) CNFs reinforced PMMA with 1% loading (1.21 and 1.24 times, respectively) (Jamaluddin et al. 2021). Thus, the Ac-CNF in this study exhibited the higher reinforcement effect (1.34 times) than the previous CNFs. This could be attributed to the high DS of 2.24, and the acquired hydrophobicity might have afforded good dispersion of Ac-CNFs in the PMMA matrix. Interestingly, when 3-(methacryloyloxy)propyltrimethoxysilylane (MPTMS) as a more compatible functional group than conventional acyl groups was introduced into bacterial CNFs, only 0.1% loading of the CNFs reinforced the tensile strength of PMMA to 1.55 times (Kono et al. 2022). In this case, they used an expensive bacterial cellulose instead of the industrial cellulose powder.

The effect of 1% CNFs on the thermal stability of PMMA was investigated by TGA of neat PMMA and composite films (**Fig. 6**). The $T_{d-5\%}$ of neat PMMA was 326°C, while those of the composite films with 1% of Ac-CNFs, TOCN, and CM-CNFs were 341, 330, and 331 °C, respectively. This result suggests that the 1% Ac-CNF incorporation is an effective filler for improvement of not only the mechanical properties of PMMA (**Fig. 5**) but also its thermal stability.

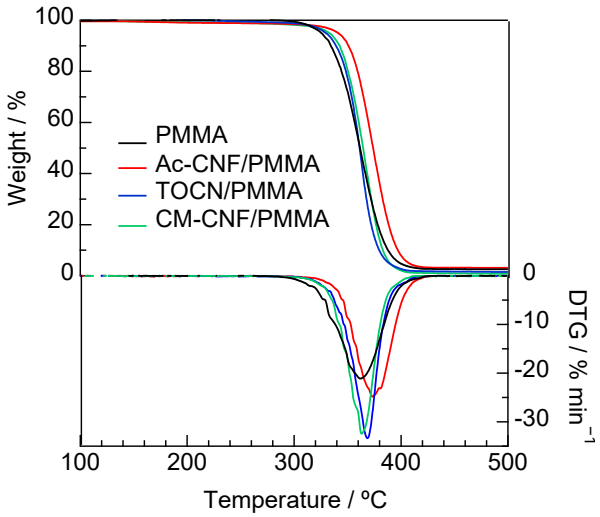

Fig. 6. TG and differential TG (DTG) curves of neat PMMA film and composite films with 1% Ac-CNFs, TOCN, and CM-CNFs.

Conclusions

A facile method for fabricating an Ac-CNF-reinforced PMMA film with high transparency was developed by exploiting the cosolvency effect of EtOH aq. in PMMA dissolution. This method offers simple procedures that do not require tedious solvent exchange process when using common organic solvents. The dope was prepared by the direct addition of EtOH to the as-prepared Ac-CNF aq. suspension, followed by dissolving PMMA at 65 ºC, adequately above UCST. The casting and drying conditions significantly affected the film morphology; that is, a uniform and transparent film was successfully fabricated by casting the dope at 65 ºC and subsequent drying it at 45 ºC for 24 h in a closed oven. The obtained composite film with 1% Ac-CNFs exhibited a high transparency comparable to that of the neat PMMA film. The reinforcing effect of 1% Ac-CNFs on the tensile strength of PMMA was the highest among the other 1% CNFs, including TOCN, CM-CNFs, and previously reported hydrophilic and hydrophobic CNFs. The incorporation of 1% Ac-CNFs also led to enhance the thermal stability of PMMA. Because the cosolvency phenomena in aqueous alcohols are not limited to PMMA but also apply to other synthetic polymers (Young et al. 1998; Asadujjaman et al. 2017), the novel methodology developed in this study is versatile for fabricating composite films consisting of other plastic materials and commercially available CNF aq. suspension.

Acknowledgements: The authors thank Dr. Masanori Yasui and Mr. Toshiaki Ito (Electron Microscope Laboratory, Research Faculty of Agriculture, Hokkaido University) for supporting our microscopic observations.

Author contributions: S.T. planed the study conception, and S.S. and Y.U. supervised the work. I.T. performed film preparation, tensile tests, UV-vis measurements, and data analysis. S.T. did TG measurements. S.S. carried out SEM observations and haze measurements, kindly supported by T.I. S.T. wrote the first draft of the manuscript, and S.S. and Y.U. revised the manuscript. All authors commented on previous versions of the manuscript. All authors read and approved the final manuscript.

Funding: This work was financially supported by a Promotion for Young Research Talent and Network from the Northern Advancement Center for Science and Technology (NOASTEC) Foundation to S.S.

Declarations

Conflicts of Interest: The authors declare no competing interest.

References

Abe K, Iwamoto S, Yano H (2007) Obtaining cellulose nanofibers with a uniform width of 15 nm from wood. Biomacromolecules 8:3276–3278. https://doi.org/10.1021/bm700624p

Ali U, Karim KJBA, Buang NA (2015) A review of the properties and applications of poly (methyl

methacrylate) (PMMA). Polym Rev 55:678–705. https://doi.org/10.1080/15583724.2015.1031377

Asadujjaman A, Ahmadi V, Yalcin M, Brummelhuis NT, Bertin A (2017) Thermoresponsive functional polymers based on 2,6-diaminopyridine motif with tunable UCST behaviour in water/alcohol mixtures. Polym Chem 8:3140–3153. https://doi.org/10.1039/c7py00539c

Cowie JMG, McEwen IJ (1974) Upper and lower critical solution temperatures in the cosolvent system acetone(1) + diethyl ether(2) + polystyrene(3). J Chem Soc Faraday Trans 1 70:171–177. https://doi.org/10.1039/F19747000171

Cowie JMG, Mohsin MA, Mcewen IJ (1987) Alcohol-water cosolvent systems for poly(methyl methacrylate). Polymer 28:1569–1572. https://doi.org/10.1016/0032-3861(87)90360-0

Daicho K, Saito T, Fujisawa S, Isogai A (2018) The crystallinity of nanocellulose: dispersion-induced disordering of the grain boundary in biologically structured cellulose. ACS Appl Nano Mater 1:5774–5785. https://doi.org/10.1021/acsanm.8b01438

Dong H, Sliozberg YR, Snyder JF, Steele J, Chantawansri TL, Orlicki JA, Walck SD, Reiner RS, Rudie AW (2015) Highly transparent and toughened poly(methyl methacrylate) nanocomposite films containing networks of cellulose nanofibrils. ACS Appl Mater Interfaces 7:25464–25472. https://doi.org/10.1021/acsami.5b08317

Fujisawa S, Togawa E, Kimura S (2018) Large specific surface area and rigid network of nanocellulose govern the thermal stability of polymers: mechanisms of enhanced thermomechanical properties for nanocellulose/PMMA nanocomposite. Mater Today Commun 16:105–110. https://doi.org/10.1016/j.mtcomm.2018.05.002

Fukuzumi H, Saito T, Iwata T, Kumamoto Y, Isogai A (2009) Transparent and high gas barrier films of cellulose nanofibers prepared by TEMPO-meditated oxidation. Biomacromolecules 10:162–165. https://doi.org/10.1021/bm801065u

Guo YN, Qiu JJ, Tang HQ, Liu CM (2011) High transmittance and environment-friendly flame-resistant optical resins based on poly(methyl methacrylate) and cyclotriphosphazene derivatives. J Appl Polym Sci 121:727–734. https://doi.org/10.1002/app.33806

Hänig J, Weller B (2021) Experimental investigations and numerical simulations of innovative lightweight glass–plastic-composite panels made of thin glass and PMMA. Glass Struct Eng 6:249–271. https://doi.org/10.1007/s40940-021-00153-x

Heiba ZK, Bakr MM, Imam NG (2016) Photophysical parameters of functional transparent polymethyl-methacrylate/double-walled carbon nanotubes nanocomposite sheet under UV-irradiation. J Inorg Organomet Polym Mater 26:780–787. https://doi.org/10.1007/s10904-016-0367-x

Isogai A (2020) Emerging nanocellulose technologies: recent developments. Adv Mater 33:1–10. https://doi.org/10.1002/adma.202000630

Jamaluddin N, Hsu YI, Asoh TA, Uyama H (2021) Optically transparent and toughened poly(methyl methacrylate) composite films with acylated cellulose nanofibers. ACS Omega 6:10752–10758. https://doi.org/10.1021/acsomega.1c00325

Joshi S, Drzal L, Mohanty A, Arora S (2004) Are natural fiber composites environmentally superior to glass fiber reinforced composites? Compos Part A Appl Sci Manuf 35:371–376. https://doi.org/10.1016/j.compositesa.2003.09.016

Kono H, Tsujisaki H, Tajima K (2022) Reinforcing poly (methyl methacrylate) with bacterial cellulose nanofibers chemically modified with methacryolyl groups. Nanomaterials 12:537–552. https://doi.org/10.3390/nano12030537

McNaught A, Wilkinson A, Chalk S (1997) IUPAC. Compendium of chemical terminology, 2nd ed. (the "Gold Book"). https://goldbook.iupac.org/terms/view/C01361. Accessed 7 Feb 2023

Moon RJ, Martini A, Nairn J, Simonsen J, Youngblood J (2011) Cellulose nanomaterials review: Structure, properties and nanocomposites. Chem Soc Rev 40:3941–3994. https://doi.org/10.1039/c0cs00108b

Nakata M (1995) Coil-globule transition of poly(methyl methacrylate) in a mixed solvent. Phys Rev E 51:5770–5775. https://doi.org/https://doi.org/10.1103/PhysRevE.51.5770

Niskanen I, Zhang K, Karzarjeddi M, Liimatainen H, Shibata S, Hagen N, Heikkilä R, Yoda H, Otani Y (2022) Optical properties of cellulose nanofibre films at high temperatures. J Polym Res 29:187. https://doi.org/10.1007/s10965-022-03019-0

Okita Y, Fujisawa S, Saito T, Isogai A (2011) TEMPO-oxidized cellulose nanofibrils dispersed in organic solvents. Biomacromolecules 12:518–522. https://doi.org/10.1021/bm101255x

Patra N, Barone AC, Salerno M (2010) Solvent effects on the thermal and mechanical properties of poly(methyl methacrylate) casted from concentrated solutions. Adv Polym Technol 30:12–20. https://doi.org/10.1002/adv.20203

Rusli R, Shanmuganathan K, Rowan SJ, Weder C, Eichhorn SJ (2010) Stress-transfer in anisotropic and environmentally adaptive cellulose whisker nanocomposites. Biomacromolecules 11:762–768. https://doi.org/10.1021/bm1001203

Shih YF, Chou MY, Lian HY, Hsu LR (2018) Highly transparent and impact-resistant PMMA nanocomposites reinforced by cellulose nanofibers of pineapple leaves modified by eco-friendly methods. Express Polym Lett 12:844–854. https://doi.org/10.3144/expresspolymlett.2018.72

Taira S, Tsuruhara M, Saito R, Koda K, Uraki Y, Konnno H, Shimamoto S (2020) Cellulose acetate with CTA I polymorph can be defibrated into nanofibers to produce a highly transparent nanopaper. Cellulose 27:4991–5001. https://doi.org/10.1007/s10570-020-03156-z

Wang L, Ando M, Kubota M, Ishihara S, Hikima Y, Ohshima M, Sekiguchi T, Sato A, Yano H (2017) Effects of hydrophobic-modified cellulose nanofibers (CNFs) on cell morphology and mechanical properties of high void fraction polypropylene nanocomposite foams. Compos Part A Appl Sci Manuf 98:166–173. https://doi.org/10.1016/j.compositesa.2017.03.028

Wolf B, Molinari R (1973) True cosolvency acetone / diethylether / polystyrene. Makromol Chem 173:241–245. https://doi.org/10.1002/macp.1973.021730118

Yano H, Sugiyama J, Nakagaito AN, Nogi M, Matsuura T, Hikita M, Handa K (2005) Optically transparent composites reinforced with networks of bacterial nanofibers. Advanced Materials 17:153–155.

https://doi.org/10.1002/adma.200400597

Yoneda S, Han W, Hasegawa U, Uyama H (2014) Facile fabrication of poly(methyl methacrylate) monolith via thermally induced phase separation by utilizing unique cosolvency. Polymer 55:3212–3216. https://doi.org/10.1016/j.polymer.2014.05.031

Young TH, Cheng LP, Hsieh CC, Chen LW (1998) Phase behavior of EVAL polymers in water-2-propanol cosolvent. Macromolecules 31:1229–1235. https://doi.org/10.1021/ma9710388